NOVEL METHOD FOR HIGH IMPEDANCE FAULT RECOGNITION BASED ON SIGNAL PROCESSING AND NEURAL NETWORK

Abdulhamid. A. Abohagar[a], Mohd. W. Mustafa[*b]

[a]*Libyan Authority for Scientific Research. Tripoli,Libya
[b]*Faculty of Electrical Engineering, Universiti Teknologi Malaysia, Johor Bahru, Malaysia

***Abstract*—**A novel hybrid method is presented in this paper, which involves the combination of radial basis function neural network RBFNN with discrete wavelet transform DWT. The proposed hybrid method specifically detects and distinguishes high-impedance fault HIF from other transient events, such as capacitor and load switching. A signal has been extracted using wavelet transform to acquire updated and accurate information from the current signal during the fault. The RBFNN classifier has been presented and used to detect and classify HIF from normal conditions to improve the protection scheme in terms of accuracy and computational time. The new approach provides a robust characterization and classification of different fault conditions in terms of a variety of fault resistance and fault location. The hybrid approach has been examined by performing extensive simulation studies, and the outputs are compared with the previous state of the art, which clearly shows the significance of the proposed method.

Keywords— High impedance fault, wavelet transform, artificial neural network

1. INTRODUCTION

Nowadays, stability and reliability have become significant concerns for power system utility. High impedance fault HIF is one of the interruptions in power systems. HIF occurs when the broken conductor falls on the ground or touches the branches of a tree, which makes the conducting surface poor, resulting in a very low current, which makes the protection devices out of order [1]. Also, the arc that regularly accompanies such faults causes fire hazards and dramatically increases the risk to human life. Hence, detecting and recognizing such faults are crucial [2]. Many different techniques have been applied to analyze HIF faults. In [3], the method has analyzed HIFs based on the fractal

theorem. Some other techniques were based on different filters, such as Fourier Transform and Kalman Filter [4].

Recently, wavelet transform has implemented for high-impedance fault detection and discrimination [5]. Other researchers have introduced new intelligent techniques such as neural networks and fuzzy logic [6-9]. Although neural network classifiers for high impedance fault have been extensively proposed, most of these studies have employed a backpropagation supervised learning algorithm; however, the backpropagation neural network has several drawbacks such as slow learning, large training sets needed, and difficulty in selecting a proper size of the network.

The application of a neuro-fuzzy learning technique based on data streams for medium-voltage power line HIF detection is presented and investigated [10]. To identify spatial-temporal patterns in the data, a variant of an evolving neuro-fuzzy network with fluctuating thresholds and a feature extraction technique based on wavelet packet transforms are considered. Wavelet families like Haar, Symlet, Daubechie, Coiflet, and Biorthogonal were studied to provide the most discriminative features for fault detection. Due to concept changes in the HIF environment, the suggested evolving neuro-fuzzy classification model has proven to be especially well-suited for the problem. The developed neuro-fuzzy model for HIF classification is parametrically and structurally adaptive to deal with the issue, which sets it apart from other statistical and intelligent approaches problems. New neurons and connections are incrementally added to the neuro-fuzzy network when necessary to identify new patterns. The suggested classifier is evaluated experimentally against other well-known computational intelligence techniques.

Although supervised machine learning techniques have demonstrated remarkable success in HIF detection, they depend on resource-intensive signal processing methods. They are ineffective when non-HIF disturbances exist and training data does not contain specific scenarios. This technique suggests a Convolutional Autoencoder framework for HIF Detection (CAE-HIFD) that uses unsupervised learning. Using cross-correlation, the Convolutional Autoencoder in CAE-HIFD learns exclusively from HIF signals, obviating the need for various non-HIF training scenarios. A novel HIF classification method based on the transformer network stacked with the convolution neural network is proposed in an MSc thesis at The University of Western Ontario, Canada [11].

Another research investigated the detection of HIF in an integrated solar photovoltaic (PV) power system using a recurrent neural network approach with long short-term memory (LSTM). The research modeled an IEEE 13-bus system in MATLAB/Simulink software for integrating 300 kW of solar PV systems for analysis. Features were extracted using (HIF, symmetrical, and unsymmetrical fault) criteria. For training and testing the classifiers, the energy value features of each phase were extracted using the Discrete Wavelet Transform signal processing technique with db4 mother wavelet. The suggested LSTM classifier identifies HIF in PV-integrated power networks with a success rate of 92.42% and an overall classification accuracy of 91.21% [12]. The prediction outcomes of the suggested methodology are contrasted with those of several well-known classifiers, including the Naïve Bayes approach, J48-based decision tree, Support Vector Machine, and K-Nearest Neighbors network. Additionally, by assessing the performance indices (PI) of the kappa statistic, precision, recall, and F-measure, the robustness of the classifier is confirmed. According to the data, the suggested

LSTM network performs noticeably better than all PI compared to the alternative method [12].

A novel technique for identifying HIFs in active distribution networks is put forth to increase the detection accuracy of HIFs. The time-frequency spectrum (TFS) is first obtained by applying the continuous wavelet transform (CWT) to the gathered zero-sequence currents under different operating conditions. The zero-sequence current signals are then denoised using an efficient algorithm called modified empirical wavelet transform (MEWT), which produces several intrinsic mode functions (IMFs). Second, the symmetric dot pattern (SDP) converts IMFs into a two-dimensional spatial domain fused image. To thoroughly examine the system's fault features, the TFS and SDP images are synchronized as inputs to a hybrid convolutional neural network (Hybrid-CNN). After achieving HIF detection using the Sigmoid function, simulation, and experimental validation are conducted. Although it cannot handle completely different network topologies, the model created in this study can be used in situations with topology variations within the same distribution network [13].

A dual-path neural network for HIF detection is proposed in research with valuable results in early 2025[14]. The model outperforms single-modality approaches by incorporating temporal and spatial data through a dual-branch architecture that processes raw zero-sequence voltage signals and their Gramian Angular Field transformations. Enhancing hyperparameter optimization, the Crested Porcupine Optimizer increases the model's generalization and adaptability to different network conditions and noise levels. The Hardware-in-the-Loop validation demonstrated the technology's practicality, which distinguished defects from normal processes with 99.70% accuracy.

This paper presents a superior technique; the method is based on the discrete wavelet transform for feature extraction using Multi-Resolution Analysis MRA. Additionally, the radial basis function RBF is a classifier that detects and discriminates HIF from similar transient events. The proposed hybrid mechanism has been compared with previous results of BPNN. The analysis shows that the proposed technique is highly reliable and accurate, with better computation time because of its fast learning capability. Therefore, the RBFNN is implemented in this study to achieve excellent performance in simplicity, accuracy, and computation time.

1.1 Modeling of High Impedance Fault

Simulating a complete model of HIF remains challenging due to its characteristics, asymmetry, and nonlinearity. The model of HIF is created and simulated (PSCAD/EMTDC), as shown in Figure 1. The model used has been discussed in detail in [**15**].

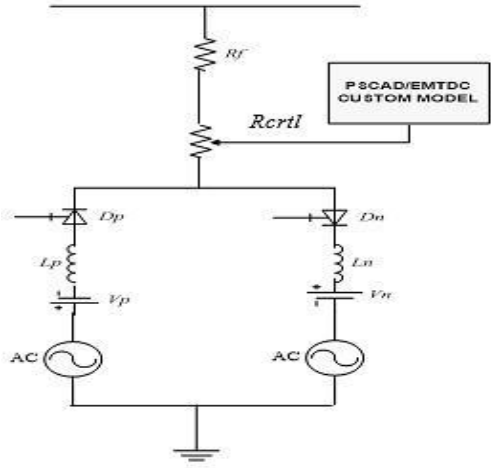

Fig 1. *High Impedance Fault Model*

1.2 Simulation System Of Case Study

This study employs the standard IEEE 6-bus transmission system to assess the effectiveness and efficiency of the proposed algorithm. Simulation were carried out using PSCAD/EMTDC software; during which various fault conditions were examined for a transmission line modelled as Bergin line with length of 100 km and a base voltage of 138 kV. The system is depicted in Figure 2, which includes of two generators, six buses, two transformer branches, and two compensation branches.

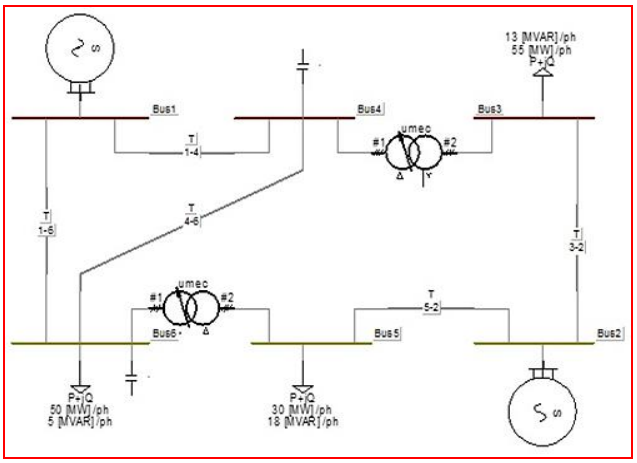

Fig 2. IEEE 6-Bus Transmission System

The important part of this study is the transmission line, so the data used for the transmission line is shown in Table 1.

Table 1. TRANSMISSION LINE DATA

line	Buses	R(pu)	X(pu)	B(pu)	V(pu)
1	1-4	0.123	0.518	0.03	1.1
2	1-6	0.08	0.37	0.01	1.15
3	2-3	0.0723	1.05	0.022	1.03
4	2-5	0.232	0.064	0.12	0.996
5	3-4	0	0.133	0.33	1.014
6	4-6	0.097	0.407	0.01	0.977
7	5-6	0	0.3	0.025	0.977

2. WAVELET TRANSFORM

Wavelet transform WT has become a computational tool for many different applications; it was established early in the 1980s and has been extensively introduced in the image processing field. Since then, it has been implemented in applications of power system engineering. Wavelets can decompose the signal in both time and frequency localization. In addition, the discrete wavelet transform considered here is easier to implement and faster than the conventional transforms. To process the data in a digital sense, the DWT is implemented here [16], and it is given by eq (1):

$$W(h,i) = \sum_h \sum_i x(i)\, 2^{-h/2} \psi\left(2^{-h} n - i\right) \quad (1)$$

The DWT for any signal can be described by two integers *h,i*, Where, $\psi(t)$ is the mother wavelet, $x(i)$

is the input time discretized signal.

In this study, the wavelet transform has categorized into three steps: DE-noising Process, Signal Decomposition, and Feature Extraction, which will explained in detail in this section.

2.1 De-Noising Process

This process has implemented in case of having a lot of noise and harmonics that may produced by switching operations, etc. The goal of this step is to avoid the adverse effect of noise and eliminate the distortions from the current signal; this process assists in improving the performance of the proposed method. There are two types of thresholds: hard and soft; here, we have selected the soft threshold, which has good mathematical properties [17].

2.2 *Signal Decomposition*

Wavelets have several mother wavelets, such as Daubichis, Coiflet, and Symmlet wavelets, are the most famous wavelet in signal processing extraction, which represent the most important characteristics of the signals. In this study, since we are working on low amplitude and short duration of high-frequency current signal, so it needs to select the most proper wavelet by implementing many simulation tests that reveal to the most suitable mother wavelet is Daubichies's wavelet four (db4), as shown in Figure3. This mother wavelet has selected because it has properties such as accurately detecting low amplitude signals with short duration and fast decay.

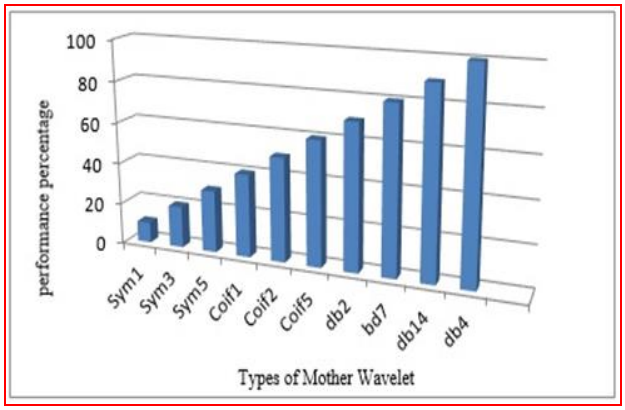

Fig 3. Percentage of different mother wavelet

This selected wavelet decomposes the signal by using filters of different cut-off frequencies to analyze the signal at various scales, where (D) is the Details coefficients, which are generated from high-pass filters, and (A) are approximations coefficients generated from low-pass filters, and this can be expressed, mathematically as refer to (2,3) [18].

$$Dj[n] = \sum_k x[n].g[2n-k] \quad (2)$$

$$A\,j[n] = \sum_k x[n].h[2n-k] \quad (3)$$

Where Dj is called details, and Aj is called Approximation, at resolution j, j = 1, 2, J; k = 1, 2, K, .K where K is filter length, after downsampling by two. In the following Figure 4, we assume that the original signal is x[n]. The signal is passed through a half-band high-pass filter HPF and a low-pass filter LPF, then the output of the low-pass filter is again divided in half and sent to the second stage. Then, the process will frequently continue until the signal is fetid to a well-known definite level.

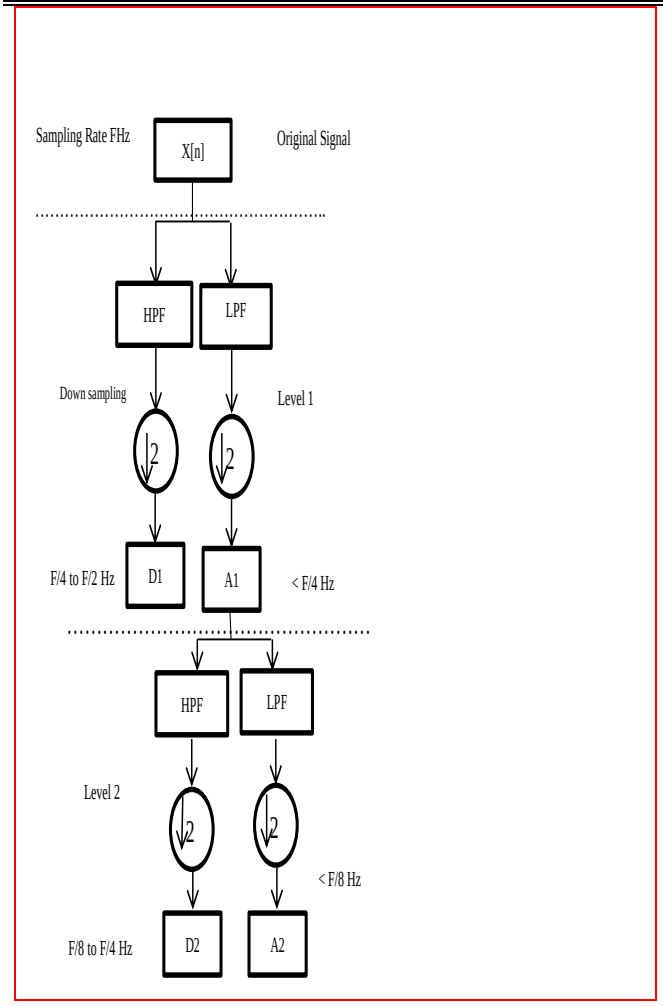

Fig 4. Implementation of MRA

2.3 Feature Extraction

The task of this process is to find distinctive parameters with significant information that can represent the features of the problem. Different wavelet signal features have been selected and calculated to overcome the neural network convergence and avoid the network's increasing size, such as Mean, Standard Deviation, Skewness, and Kurtusis, as illustrated in Table 2. The main advantage of this process is reducing the size of the neural network and remaining essential features of the original signal. Where these features are estimated from the following equations:

$$\eta = \frac{1}{N}\sum_{N=1}^{N}(x[n]) \quad (4)$$

$$\sigma = \left(\frac{1}{N}\sum_{N=1}^{1}(x[n]-\eta)^2\right)^{0.5} \quad (5)$$

$$\gamma = \frac{1}{N\sigma^3}\sum_{N=1}^{1}(x[n]-\eta)^4 \quad (6)$$

$$\mathcal{K} = \frac{1}{N\sigma^4}\sum_{N=1}^{1}(x(n)-\eta)^4 \quad (7)$$

Where η is Mean, σ is Standard Deviation, γ is Skewness, and κ is Kurtosis.

Table 2. Sample of Feature Coefficients

Mean	Standard deviation	Skewness	Kurtosis
1.2762	4.491	0.4876	1.9599
3.32E-04	0.0056	-2154	27.5292
0.0016	0.0241	0.237	13.0252
1.2762	4.491	0.4876	1.9599
-0.1088	3.4165	0.2424	1.9912
5.75E-04	0.004	4.0834	26.6995
0.0018	0.0239	0.2033	13.7734
-0.1088	3.4165	0.2424	1.9912
-0.1937	2.8588	0.2499	1.937
4.35E-04	0.0033	4.4564	32.7463
0.0012	0.0232	0.2135	15.6313
-0.1937	2.8588	0.2499	1.937
-0.2155	2.5604	0.2627	1.895
2.39E-04	0.0029	3.7595	31.0865
0.0015	0.023	0.1859	16.0272
-0.2155	2.5604	0.2627	1.895
-0.2239	2.3845	0.2709	1.8641
3.09E-04	0.0025	4.0253	27.9546

0.0015	0.0232	0.1474	15.7896
-0.2239	2.3845	0.2709	1.8641
-0.228	2.2717	0.2757	1.8422
1.76E-04	0.002	4.1446	31.9328
0.0013	0.023	0.1673	16.1559
-0.228	2.2717	0.2757	1.8422

3. RADIAL BASIS FUNCTION NETWORKS

Neural networks have become one of the great technologies in all applications, such as engineering and science, which involves developing a series of artificial neural networks. However, the backpropagation neural network (BPNN) is the typical procedure for a multi-layer neural network. It is based on a steepest descent approach to minimize the error prediction. Although it's used in many applications, there are several disadvantages, such as slow learning, the need for vast training sets, and difficulty in selecting the optimal network size.

The radial basis function RBF consists of three layers, as shown in Figure 5. The first layer is the input layer, which is not weighted; the second layer is the hidden layer, which is weighted and composed of Kernel nodes that are based on radial basis functions; the last layer is the output layer, which is just a simple summation. The radial basis function network has distinctive advantages, such as being efficiently designed and having very good generalizations that make it suitable for this study. [19-20].

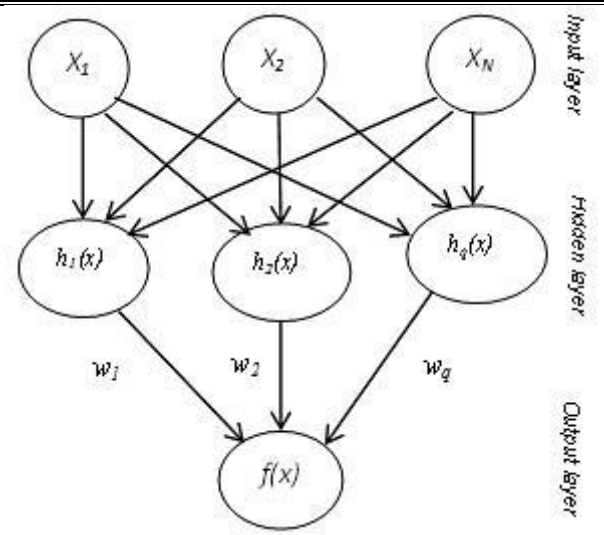

Fig 5 Basic Architecture of RBFN

Since the Gaussian function is the most popular RBF function and is adopted here and presented by [21], as referred to (8, 9)

$$G_p(x) = exp(-Z_p/w_p^2) \quad (8)$$

$$Z_p = \sum_{k=1}^{N}(C_{pk} - X_K)^2 \quad (9)$$

Where the input is represented by the N-dimensional vector X = (X1; X2; …XN), Gq(x) is the response function of the kernel unit, and cp and wp are the center and width of the pth unit.The selection of neural network size remains a topic of discussion. The proper choice for complex systems such as high-impedance fault detection could be two independent and two hidden layers [22]. The input of neural networks will explained in detail in the next issue.

4. RESULTS AND DISCUSSION

In the presented technique to validate the proposed algorithm, a vast number of HIF and

other transient events cases have been simulated and investigated using PSCAD/EMTDC and MATLAB software as considered here, the single line to ground fault is adopted, and the fault is occurred in phase A, at transmission line T3-2, with different value of fault resistance and other location of fault along the transmission line.

After the signal is generated and data is collected, we need to decompose the signal, preprocess the data, and filter the undesirable noise to reduce the amount of data, decreasing the dimension size. In this paper, as we mentioned, wavelet transform has applied for the feature extraction, and by Db4, the mother wavelet signal has decomposed into four levels, three detailed and one approximation coefficient, as shown in Figures 6 and 7.

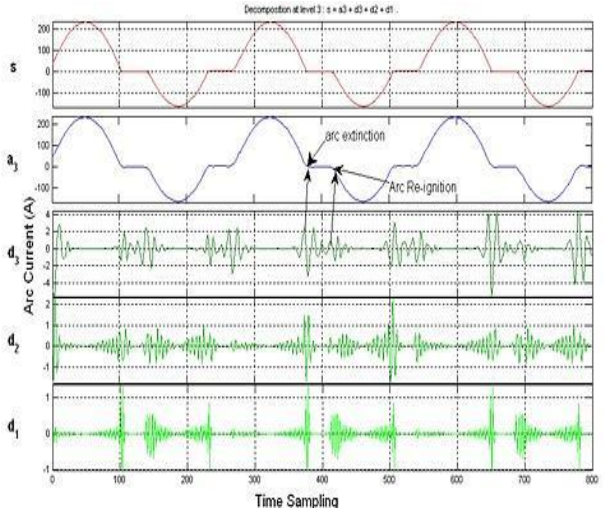

Fig 6 HIF Current Detail Coefficients at Level 3

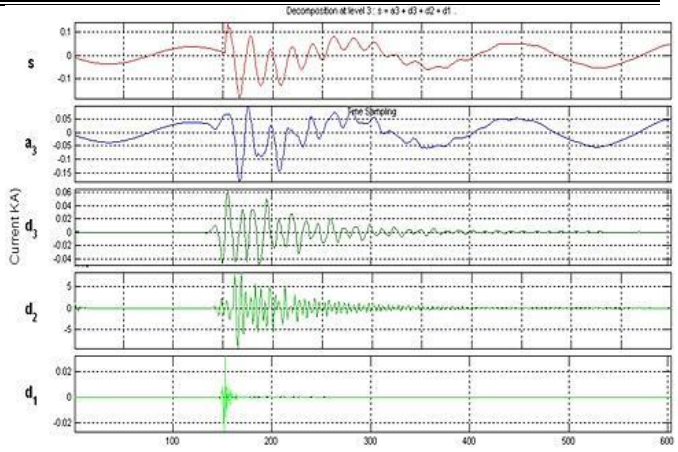

Fig 7. Capacitor Switching with Detail Coefficients at Level 3

Figures 6 and Figure 7 clearly show HIF has caused many fluctuations with a certain amplitude. Before the fault initiated, the values of detail were almost zero, and once the fault occurred, the values changed and went up for a short time, which it can be observe, that the current signal under HIF-Arc condition goes through three details coefficients (d1-d3) and one approximation a3, from the details (d1-d3) it can be clearly seen that the large spike with certain amplitude is appeared at fault occurrence. Hence, the distorted signal is evidence of arc extinction and re-ignition, considered the most important feature to recognizing high impedance faults and discriminating it from other regular operations

The input data based on the four features of the high impedance fault and capacitors switching: mean, standard deviation, Skewness, and Kurtosis. Here, we have two conditions, fault and no-fault, so the feature vector will be a dimension of 28×4, which is 196 samples used for RBF training to discriminate the fault condition from the normal one. The target consists of two classes, which are 1 for HIF and 0 for everyday situations. After normalizing the data, the vectors were distributed into three groups: 60% for network training, 30% used for testing, and the rest of the 10% for validation. Figure 8 shows the training performance of RBFNN.

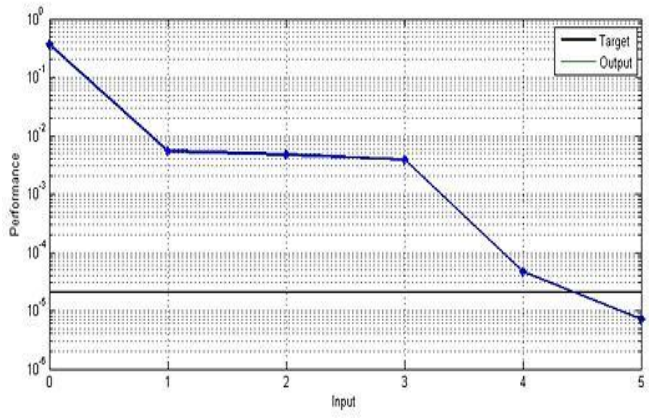

Fig 8. RBFNN Training Performances

The training performance nearly hit the goal within less than five epochs only, which gives excellent performance with a computational time of 0.085 s, which is the main advantage of the fast learning capability of RBF. In addition, the error during the training process is tiny and satisfied, which reached 0.00048 within the first five epochs, as shown in Figure 9.

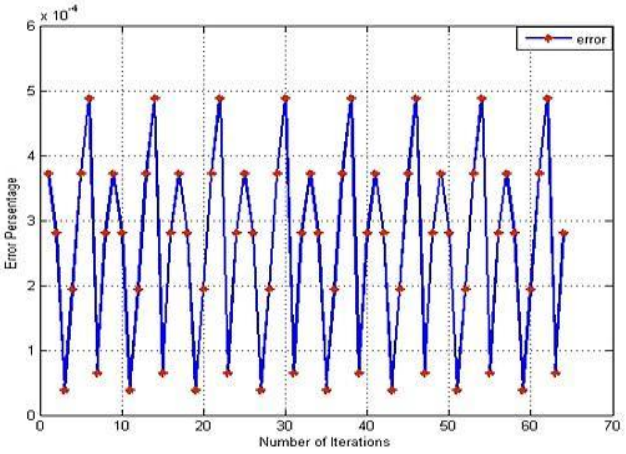

Fig 9. Errors of RBFNN training

This is to approve the proposed algorithm's success and prove that the proposed algorithm has predicted the input with accuracy. The sensitivity test is employed here by receiver operator characteristic roc; this curve is a plot used to assess the test's discriminatory power quality using sensitivity and specificity data. Figure 10 shows the roc.

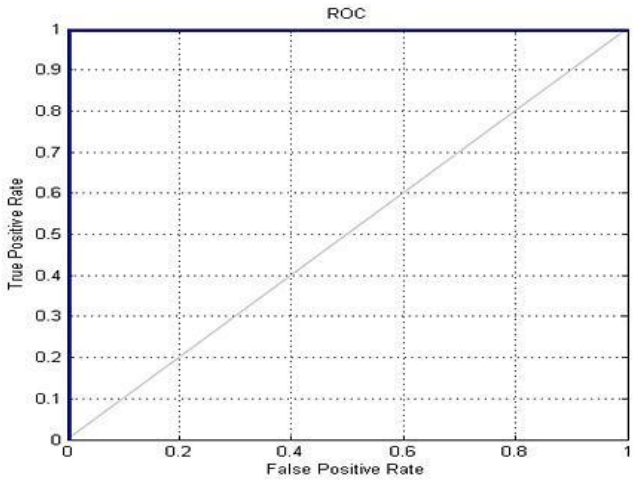

Fig 10. ROC Curve of WRBFNN Testing and Validation

Figure 10 shows us the sensitivity test of the proposed algorithm. It is clear from the curve that it strictly hits the actual positive rate, which gives a perfect for overlapping, and the neural network has predicted the input with great accuracy of almost ≈ 100%.

4.1 Comparison And Analysis

The proposed WRBFNN approach has been compared with the state-of-the-art WBPNN approach, and the same data sets have been utilized during the evaluation process. The BPNN Training performance is plotted in Figure 11, which contains three lines for the normalized input, training validation, and testing performance

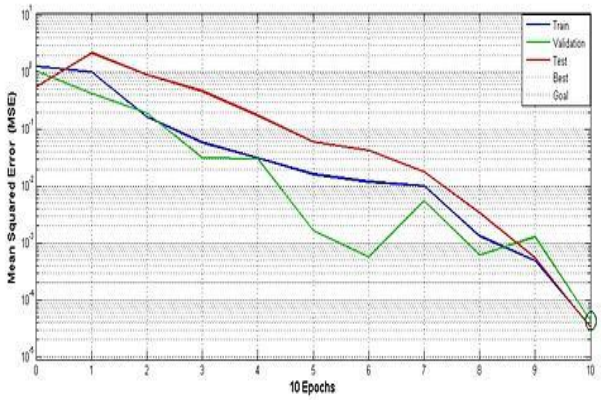

Fig 11. BPNN Training Performances

Additionally, from Figure 12, we can indicate that the training performance does not hit the goal exactly with a validation performance of 0.00427 at 10 epochs, which means that the neural network did not recognize the inputs very well.

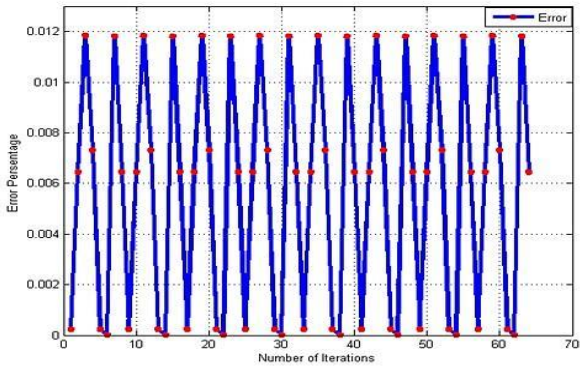

Fig 12. Errors of BPNN training

The result here is still satisfactory, and the error, as shown in Figure 12, was acceptable, attaining 0.011 within the first five iterations. Moreover, the sensitivity test of the BPNN model is plotted in Figure 13, and it clearly shows that the neural network did not exactly achieve the required. However, it is still acceptable because it shows better up to 96% accuracy. The accuracy test is measured here by the area under the ROC curve, in which an area of precisely 1 represents a perfect test and high accuracy, and an area of 0.5 represents a worthless test and less accuracy.

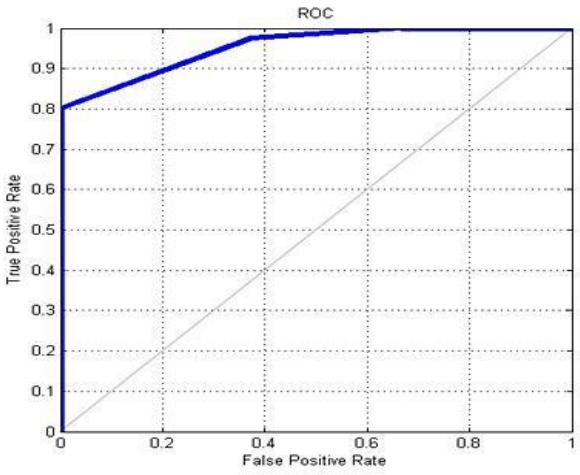

Fig 13. ROC Curve of WBPNN Testing and Validation

The output of high impedance fault and capacitor switching events has been stated in Table 3, which are attained while testing and performing simulation results.

TABLE 3. Output of Neural Network Test

Events	Desired Output	Actual Output
HIF	1	1.0021
HIF	1	0.8932
HIF	1	0.9765
HIF	1	1.06
HIF	1	1.004
HIF	1	.0904
HIF	1	1.0141
HIF	1	1.0712
HIF	1	1.00519
HIF	1	1.08
Capacitor Switching	0	0.0019
Capacitor Switching	0	0.00036
Capacitor Switching	0	0.0031
Capacitor Switching	0	0.097
Capacitor Switching	0	0.006
Capacitor Switching	0	0.00048

Consequently, if we compare the performance of the proposed WRBFNN with the WBPNN in terms of accuracy and computational time, it is clear from the results that WRBFNN achieved perfect performance. Since high impedance arcing fault is a fast transient event, the protection scheme must indicate it quickly. In addition, some other transient events behave as such faults; hence, the protection scheme must classify these events from HIF to avoid conflict in decision-making.

The robustness of the WRBFNN proposed approach in classification accuracy is also demonstrated through the results presented in Figure 14, which clearly shows that the output

data revealed the high impedance fault appeared at one, indicating fault occurrence. In addition, the features of customary conditions, such as capacitor switching, appeared at 0, which stated no fault conditions.

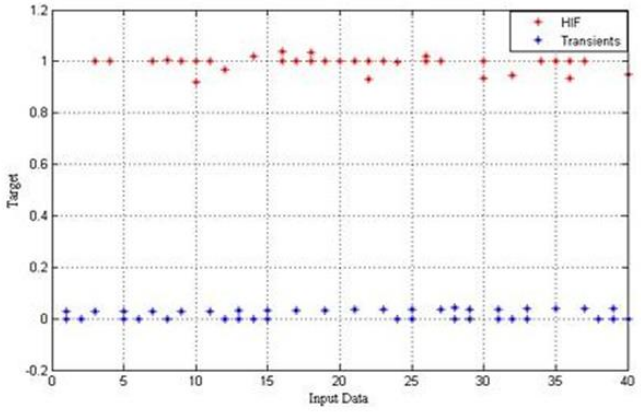

Fig 14. High-impedance fault classification

As evidenced by Figure 14, the presented technique is robust and reliable for high-impedance fault detection and classification with very high accuracy, and this can develop a new protection scheme based on the protection logic to enhance the stability and reliability of power system networks. Figure 15 shows the flow chart of the proposed protection scheme.

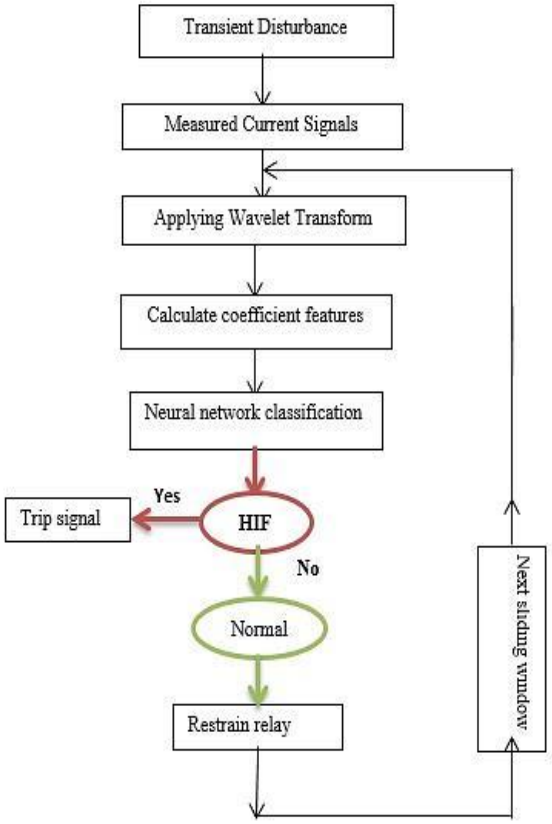

Fig 15. Relay logic based on wavelet transform and neural network

5. CONCLUSION

A novel technique using discrete wavelet transform incorporating artificial neural networks is presented; the method is applied to detect and characterize the single line to ground high impedance fault from normal conditions. The proper selection of Daubechies4 (db4) is adopted as a mother wavelet because of its ability to extract useful information during a fault condition. Coefficients of faulted current signal and other customary conditions are calculated and used for fault detection in the decision algorithm.

The presented approach has shown high success in distinguishing the faulted signal from normal conditions with high accuracy, which is evidence

of the quality of the algorithm combination. Analysis and comparison of the performance of two types of neural networks, BPNN and RBFNN, have been presented. The extensive results show that RBFNN performs better than regular BPNN in accuracy and computational time. Further work includes considering a comprehensive power system network and different types of faults, such as line-to-line and double line-to-ground faults, for an alternative protection scheme, which can be implemented in a real power system.

REFERENCES

[1] Tengdin J, Westfall R, Stephan K. High-Impedance Fault Detection Technology. Report, PSRC working group D15, 1996.

[2] Aucoin M, Russell BD, Benner CL. "High impedance fault detection for industrial power systems", In: IEEE 1989 Industry Applications Society Annual Meeting; 1-5 October 1989; San Diego, California, USA: IEEE. pp. 1788–1792.

[3] Michalik M, Rebizant W, Lukowicz M, Lee S, Kang S. "High-impedance fault detection in distribution networks with use of wavelet-based algorithm", IEEE Transactions on Power Delivery, 2006; 21: 1793 – 1802.

[4] Girgis A, Chang W, Makram E. "Analysis of high-impedance fault generated signals using a Kalman filtering approach", IEEE Transactions on Power delivery, 1990; 5: 1714-1724.

[5] Chul-Hwan Kim, Hyun Kim, Young-Hun KO, Sung-Hyun Byun, Aggarwal RK, Johns AT. "A novel fault-detection technique of high-impedance arcing faults in transmission lines using the wavelet transform", IEEE Transactions on Power Delivery, 2002; 17: 921 - 929.

[6] Sedighi AR, Haghifam MR, Malik OP. "Soft computing applications in high impedance fault detection in distribution systems", Electrc POW Syst Res 2005, 76: 136-144.

[7] Baqui I, Zamora I, Mazón J, Buigues G. "High Impedance fault detection methodology using wavelet transform and artificial neural networks", Electr Pow Syst Res, 2011; 81: 1325–1333.

[8] Etemadi AH, Sanaye-Pasand M. "High-impedance fault detection using multi-resolution signal decomposition and adaptive neural fuzzy inference system", IET Gener. Transm. Distrib, 2008; 2: 110–118.

[9] Yang MT, GU JC. "Using wavelet transform and neural networks detection high impedance fault", International Journal of Power and Energy Systems, 2007; 27: 2872-280.

[10] Silva, S., Costa, P., Santana, M., & Leite, D. (2020). Evolving neuro-fuzzy network for real-time high impedance fault detection and classification. Neural Computing and Applications, 32, 7597-7610.

[11] Rai, K. (2021). Deep Learning for High-Impedance Fault Detection and Classification (Master's thesis, The University of Western Ontario (Canada)).

[12] Veerasamy, V., Wahab, N. I. A., Othman, M. L., Padmanaban, S., Sekar, K., Ramachandran, R., ... & Islam, M. Z. (2021). LSTM recurrent neural network classifier for

high impedance fault detection in solar PV integrated power system. IEEE access, 9, 32672-32687.

[13] Wang, C., Feng, L., Hou, S., Ren, G., & Lu, T. (2024). A High-Impedance Fault Detection Method for Active Distribution Networks Based on Time–Frequency–Space Domain Fusion Features and Hybrid Convolutional Neural Network. Processes, 12(12), 2712.

[14] Ning, K., Ye, L., Song, W., Guo, W., Li, G., Yin, X., & Zhang, M. (2025). A Dual-Path Neural Network for High-Impedance Fault Detection. Mathematics, 13(2), 225.

[15] Abdulhamid A.A, Mohd WM. "New Combined model of high impedance arcing fault in overhead transmission system", In PES conf. Asia; 2-4 April 2012, Phuket, Thailand. IASTED. pp. 38-42.

[16] Walker JS. A Primer on Wavelets and Their Scientific Applications. 2nd ed. New York, USA: Taylor & Francis Group, 2008.

[17] Donoho DL. "De-noising by soft threshold", IEEE Transaction on Information Theory, 1995; 41: 613-627.

[18] Robi P. "The story of wavelets", In IMACS/IEEE CSCC, 4-8 July 1999 Athen, Greece. pp. 5481-5486.

[19] K.Warwick, R.Craddock. "An introduction to radial basis functions for system identification. A comparison with other neural network methods", In IEEE Decision and Control Proceedings Meeting, 11-13 December 1996; Kobe, Japan: IEEE. pp. 464–469.

[20] Orr MJL. Recent advances in radial basis function networks, Technical report, Edinburgh University, 1999.

[21] Moravej Z, Vishwakarma DN, Singh SP. "Application of radial basis function neural network for differential relaying of a power transformer", Computers & Electrical Engineering 2003; 29: 421–434.

[22] Sontage ED. "Feedback stabilization using two hidden layer nets", IEEE Transaction on neural networks 1992; 3: 981-990.